Academia Journal of Environmental Science 6(8): 185-193, August 2018
DOI: 10.15413/ajes.2018.0131
ISSN: ISSN 2315-778X

Research Paper

"Characterization of industrial pollutant waste materials and clays for possible use as reinforcement in aluminum matrix composite"

Accepted 23rd August, 2018

L. Pino-Rivero[1]*, J. E. Hernández-Ruiz[2], E. Villar-Cociña[3], and A. Alujas Díaz[4]

[1] West Coast University. Miami Campus. 9250 NW 36th Street. Doral, Florida. 33178
[2]Dpto. de Física. Universidad Central de Las Villas, Carretera a Camajuaní km 5 y ½. Sta. Clara 54 830. Villa Clara, Cuba.
[3]Facultad de Química-Farmacia. Universidad Central de Las Villas, Carretera a Camajuaní km 5 y ½. Sta. Clara 54 830. Villa Clara, Cuba.

*Corresponding author. E-mail: lazaropinorivero@gmail.com.

ABSTRACT

At present, there is growing interest in the investigation of economic options for the development of aluminum matrix composites. In this context, the characterization of a cane bagasse ash from a Cuban clay, both in its natural state and after being calcined for 4 h at 1000°C, for its possible use as a reinforcement material in matrix composites of aluminum (AMCs), is described. The ash was collected directly from the boiler of the turbogenerator of the "Luis Arcos Bergnes" plant in Camajuaní and the clay is a kaolinite from an area near to the town of Miller, both in the province of Villa Clara. Using X-ray diffraction (XRD), X-ray fluorescence (XRF) and scanning electron microscopy (SEM), it was observed that the ash is composed mainly of silicon (around 80%), expressed as SiO_2, and that the phases present are mostly cristobalite and tridymite. In the case of clay, in addition to these characterization techniques, thermogravimetric analysis (DTG) was also used. The comparative study of natural and calcined clay showed that quartz, magnesium-hornblende, diopside, albite and muscovite phases are present in the latter. Most of the phases present in the ash and calcined clay are typical of high hardness ceramic materials, which gives these two materials suitable properties to be used as reinforcements in AMCs and other metal matrix composite materials.

Key words: Characterization, composites of aluminum, reinforcement.

INTRODUCTION

Since the 80s of the last century, great attention has been paid towards the study of AMCs owing to their good weight-resistance relationship along with their good mechanical-tribological properties (Lloyd, 1994; Itskos et al., 2011). Even though the costs of AMCs are relatively lower than the rest of the metallic matrix composites (MMCs) (Surappa, 2003), the search for economic options in the development of these materials was a problem of scientific-technical interest in the past (Lloyd, 1994; Kamat et al., 1989) and it is at present (Zuhailawati et al., 2007; Alaneme and Adewuyi, 2013; Włodarczyk-Fligier et al., 2008). Among these options, bagasse ash, from sugarcane, rice husk and bamboo leaves among other ash from agroindustry waste (Alaneme and Adewuyi, 2013; Lancaster et al., 2013; Anas and Khan, 2015; Saravanan and Senthilkumar, 2014; Fatile et al., 2014; Subrahmanyam et al., 2015) and natural materials (Zuhailawati et al., 2007; Jyothi and Bharath Kumar, 2015), is used as materials of reinforcement in the AMCs. The use of these ashes as reinforcement materials has been supported by studies that show that there is a high content of silica (SiO_2) and / or alumina (Al_2O_3), as well as the presence of phases of the ceramic type (Alaneme and Adewuyi, 2013; Villar-Cociña et al., 2013; Asavavisithchai and Tantisiriphaiboon, 2009), necessary for reinforcement materials in aluminum compounds.

The sugarcane bagasse ash (SCBA) is a residue of the Cuban sugar industry that causes disposal problems. In addition, its dispersion in the environment pollutes the air and affects human health. As a result, the use of SCBA and other ash from agroindustry waste, as a reinforcing material in AMCs, has become an effective alternative, since with them composites with good properties are obtained at a lower cost and at the same time it is valued as a waste, contributing directly to reducing the environmental burden (Lancaster et al., 2013).

On the other hand, within the classification of ceramic materials can be found among others silica sand and natural clays (Brindley and Brown, 1980). Clays of different types abound in Cuba and particularly in the central region of the country, where the Miller deposit is located.

The purpose of the present study was to describe the characterizations of a bagasse ash from sugarcane, coming from the boiler of a Cuban sugar mill and a Cuban natural clay (CNC), to evaluate its potential use as a material of reinforcement in AMCs.

MATERIALS AND METHODS

Characterization methods

The used in these studies was collected directly from the steam boiler of the sugar mill "Luis Arcos Bergnes" in Camajuani, Villa Clara, while CNC was obtained from a deposit near the town of Miller, also in Villa Clara.

The SCBA and the CNC were grounded in a ceramic ball mill with rotation frequency of 150 rpm for 60 min and then sieved. The particles that were finally used in the experiments correspond to the fractions that were collected below 150 µm.

For evaluation of the clay, two types of samples were prepared, one sample was clay in its natural state (CNC) and the other calcined (CCNC) for 4 h at a temperature of 1000°C and then left to cool slowly inside the oven by itself.

In the case of the SCBA, the particle distribution was determined using a particle size analyzer by laser diffraction (Malvern Mastersizer Particle Size Analyzer and Mastersizer Software long bed Version 2.19) with deionized water and dispersed particles by ultrasonic agitation for 60 s. The chemical composition of both materials was determined by X-ray fluorescence spectroscopy (XRF). A Phillips PW1400 spectrometer with Rh tube, at 30 kV and 60 mA was used. The mineralogical composition of the two materials under study was determined by means of X-ray diffraction (XRD) using a Phillips MPD 1880 diffractometer. Cu Kα radiation was used, and the identification of the phases was carried out using the PAN- databases. ICSD (2016) (PANanalytical Inorganic Crystal Structure Database) and PDF-2 of ICDD (2016) (Powder Data File of International Center for Diffraction Data). In the case of clay, samples of the CNC and the CCNC were analyzed.

As regards the CNC, thermogravimetry study (DTG) was carried out. A Perkin-Elmer DTA7 and a Perkin-Elmer TGA7 thermobalance were used. Both studies were conducted in oxygen atmospheres increasing the temperature up to 1000°C with a speed of 10°C/min. The morphological study was carried out using scanning electron microscopy (SEM) techniques. As regards the SCBA, a FEI Quanta 600 FEG microscope was used, while in the case of the clay, only samples from the CCNC were studied and as a result, a FEI Quanta 200 FEG model microscope was used. In addition, in this case, microprobe analyzes were performed at selected points in the samples.

RESULTS AND DISCUSSION

Results of the characterization of cane bagasse ash

Chemical composition of SCBA

The chemical composition of the SCBA, obtained by XRF, is shown in Table 1. The main oxide in the composition of the SCBA is silicon dioxide or silica (SiO_2) with 79.9% of the total mass, followed by potassium oxide (K_2O), phosphorus oxide III or phosphate (P_2O_5) and calcium (CaO). The rest of the oxides, such as iron oxide III (Fe2O3), magnesium oxide (MgO) and aluminum oxide or alumina (Al_2O_3), are present in smaller amounts, so that about 80% of the mass of SCBAB corresponds to silicon dioxide. According to these results, the SCBA has in a first approximation possibilities to be used as reinforcement material in AMCs.

Mineralogical composition of the SCBA

Using XRD techniques, the mineralogical composition of the SCBA was determined. Figure 1 shows that SCBAB is formed by cristobalite (SiO_2) as the main compound with cubic crystalline structure, followed by tridymite beta (hexagonal phase of SiO_2).

The presence of cristobalite can be an indication that the temperature in the boiler reaches about 1000°C or more. The presence of this phase is the result of the transformation process of amorphous to crystalline silica that takes place at a high calcination temperature in the boiler. The wide, weak band located between 15 and 350 (2 theta) is a sign of the presence of amorphous matter.

Traces of magnesium and potassium silicate ($K_2MgSi_5O_{12}$) and peaks attributed to carbon were also detected. The presence of carbon can be explained by the incomplete combustion of the bagasse. The presence of calcium and magnesium phosphate (Ca_2.81Mg0.19 $(PO_4)_2$) is not excluded, which is possible because phosphorus can be found among the most common nutrients of the earth, which can form different compounds with other elements present in sugar cane. The most abundant phases in SCBAB include cristobalite and tridymite, allotropic forms of silicon dioxide (SiO_2). This, together with the presence of silicates, gives the SCBA broad perspectives for its use as a ceramic reinforcement material in the manufacture of MMCs, particularly in AMCs.

Table 1: Chemical composition of SCBA.

Oxides	SiO_2	K_2O	P_2O_5	CaO	Fe_2O_3	MgO	Al_2O_3	Na_2O	TiO_2	Otros	LOI
m; %	79.9	5.14	4.04	3.41	2.11	2.03	1.49	0.25	0.12	0.76	075

LOI: Lost of Ignition.

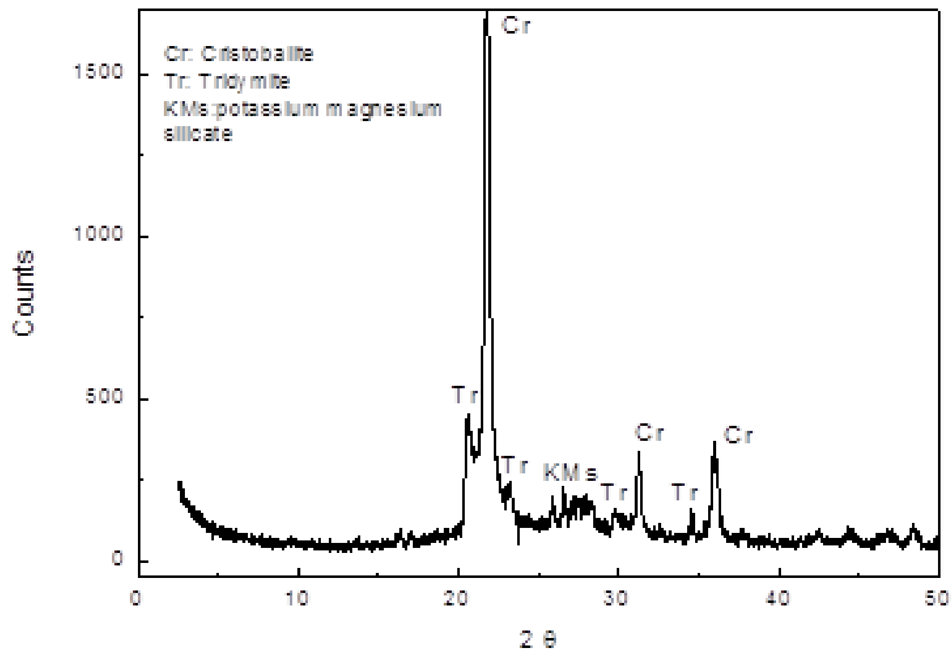

Figure 1: X-ray diffraction pattern of the SCBA.

Morphological aspect of the SCBA

It is well known that the morphology and structure of the ash depends directly on the incineration process and the temperature that is reached. Figure 2 shows the images of the morphological study carried out by SEM of the SCBA. The micrograph of Figure 2a shows the morphology of the SCBA particles with a heterogeneous mixture of cristobalite particles and particles of irregular shape, porous and smooth surface, typical of organic materials. While the other micrographs (Figure 2b and c) show the layered structures and characteristic porosity of the cristobalite particles.

Distribution and size of the SCBA particles

Figure 3 shows the particle size distribution of the SCBA, observing that such distribution is variable. According to the granulometric curve, the ash has a fine granulometry with grain diameter of about 0.7 to 130 μm and average size (D50) of 34.97 μm.

Results of clay characterization

Characterization of clay in its natural state

The chemical composition of the CNC obtained by XRF is shown in Table 2. The main oxide in the composition of the CNC is silicon dioxide or silica (SiO_2) with 43.89% of the total mass, followed by aluminum oxide or alumina (Al_2O_3) and iron oxide III (Fe_2O_3). The rest of the oxides are present in smaller amounts. As can be seen, the molar ratio SiO2 / Al_2O_3 is approximately 2: 1.

The phasic characterization of the CNC by XRD techniques allowed the determination of the presence of montmorillonite, illite and kaolinite, as shown in Figure 4. According to the chemical composition presented and the results of the XRD, the clay studied, according to the criteria of Wade and Mattox (1976) can be classified as a kaolinite. The comparative analysis of the DTG curve of the CNC with the patterns for kaolinite, illite and montmorillonite is shown in Figure 5.

As can be seen, the DTG curve of the CNC presents the common characteristics of normal clays. Among them, the

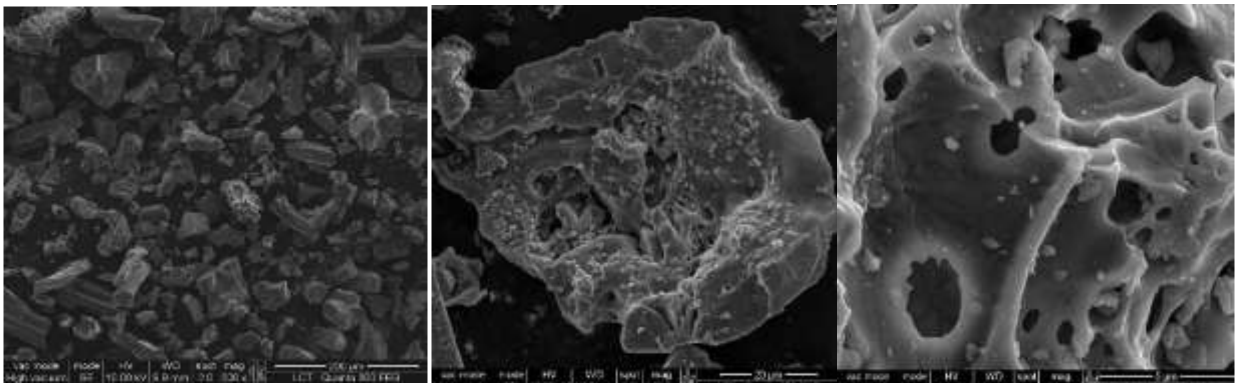

(a) (b) (c)

Figure 2: SEM micrographs of the SCBA: (a) General morphology; (b) and (c) Appearance of the cristobalite particles.

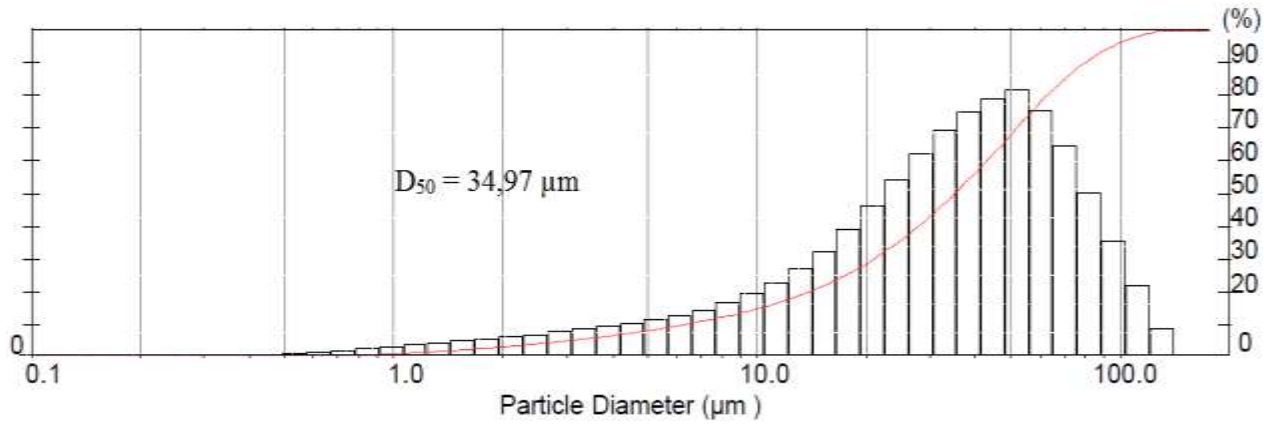

Figure 3: Particle size distribution of the SCBA.

Table 2: Chemical composition of the CNC by FRX.

Oxides	SiO_2	Al_2O_3	Fe_2O_3	CaO	Na_2O	K_2O	MgO	MnO	SO_3	others	LOI
m; %	43.89	24.73	11.13	1.38	1.99	1.10	2.63	0.14	0.08	3.11	9.82

LOI: Lost of Ignition.

loss of interlaminar water occurs in the range of 50 to 200°C, which could indicate the presence of montmorillonite (observe in the standard curve for montmorillonite as this effect appears), while the dehydroxylation process occurs in the range of 400 to 650°C, which is characteristic of kaolinites (note this effect in pure kaolinite). These results agree well with the identification of crystals by XRD. However, while the presence of illite appears on XRD, the analysis by DTG does not indicate its presence, since the endothermic peak observed in the illite pattern is absent. This is probably due to the fact that the illite phase is present in small quantities and its signal is overlapping with that of the kaolinite forming a broad band.

Upon further analysis of the DTG curve for the CNC (Figure 6), it can be inferred not only the loss of the waters of hydration and constitution, but also the destruction of the crystal lattice of the kaolinite and the fusion of those fewer refractory components. It was observed an endothermic effect below 100°C related to the loss of surface moisture, a less marked endothermic effect of above 200°C related to the loss of water from the interlaminar spaces in the kaolinite and another more marked endodermal effect approximately between 350 and

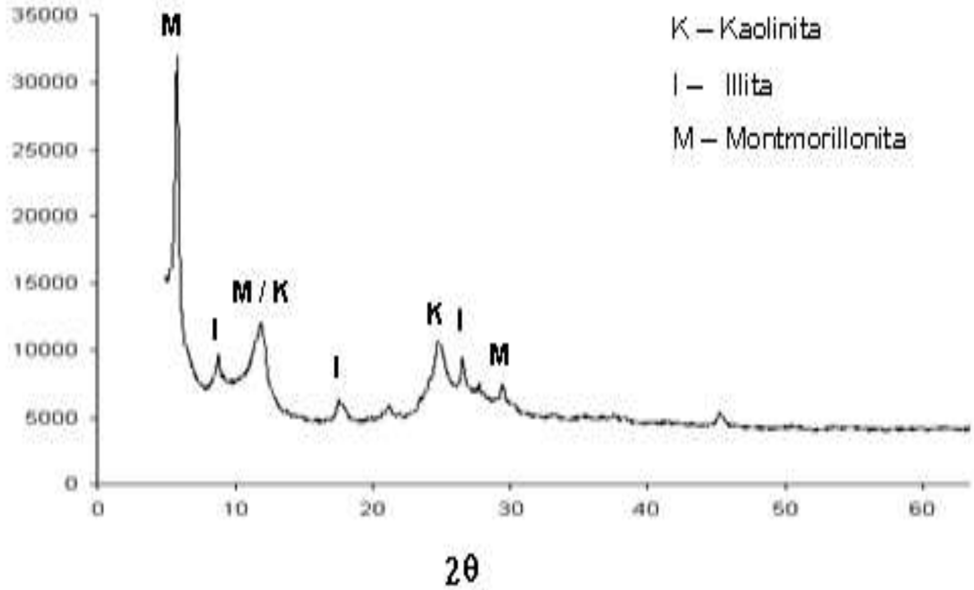

Figure 4: X-ray diffraction pattern of the CNC.

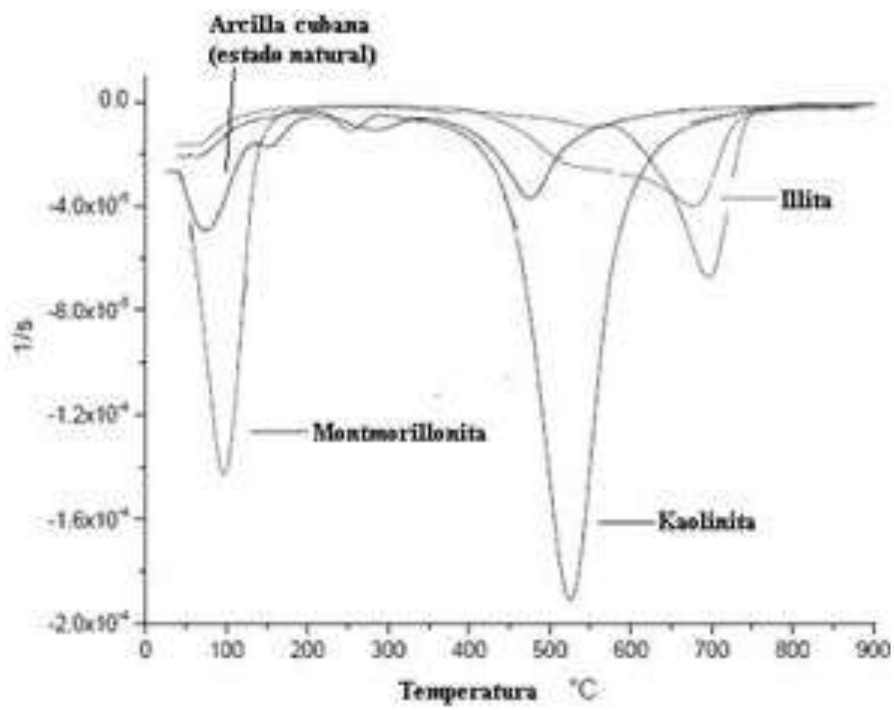

Figure 5: DTG curve for CNC.

750°C, which corresponds to the loss of hydroxyl water (constitution), causing the destruction of the crystal lattice of the kaolinite.

As can be seen in the DTG, above 900°C, no changes were observed in the clay studied, so it was decided to subject it to a process of calcination for 4 h at a temperature of 1000°C and then allowed to cool slowly inside of the furnace, with the objective of studying the products of the topochemical reactions that occur during the calcination process, which could lead to ceramic structures of high refractoriness and hardness, such as those needed to reinforce luminum composite materials.

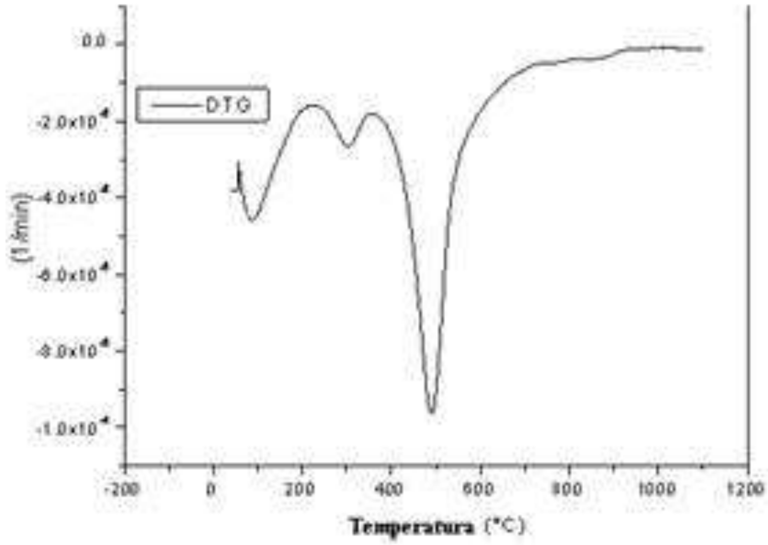

Figure 6: DTG of CNC.

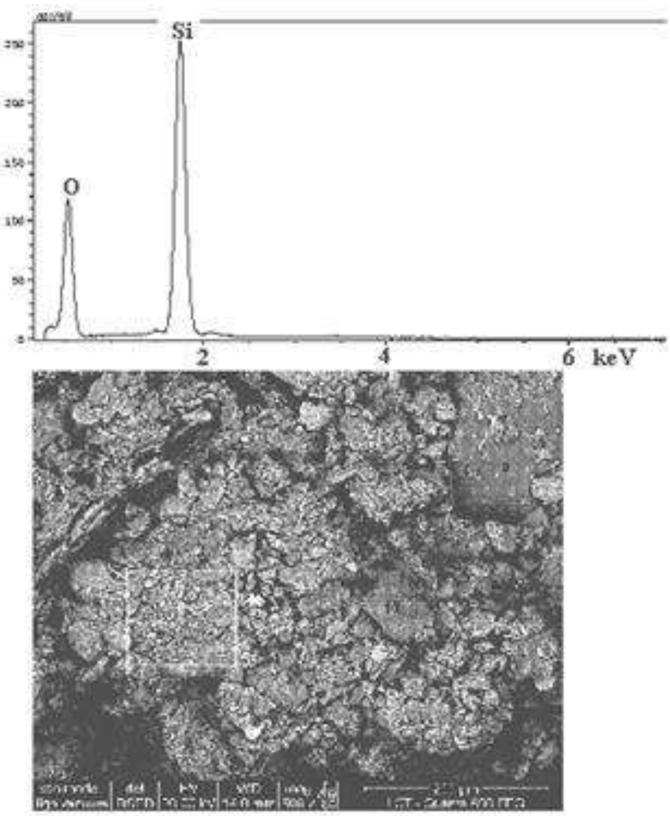

Figure 7: SEM of CCNC.

Characterization of calcined clay

The phasic characterization by XRD of the CCNC for 4 h at 1000°C showed the presence of quartz, magnesium-hornblende, muscovite, diopsidium and albite.

Figure 7 shows the micrograph of a sample of the CCNC obtained by SEM and the microprobe analysis corresponding to a quartz grain. As can be seen from the chemical composition and the morphology of the mineral, this point corresponds precisely to quartz, a phase detected

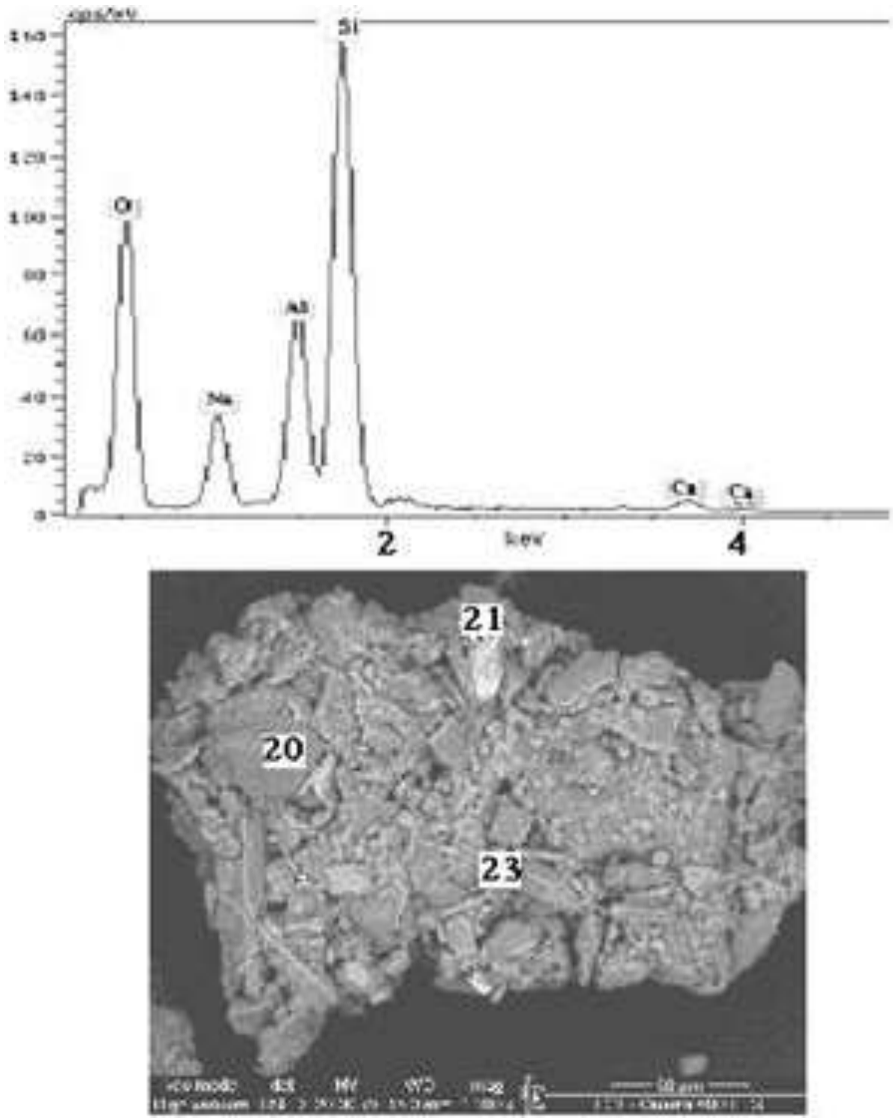

Figure 8: Point 21 correspond to quartz grain and point 23 is hornblende grain.

in the CCNC by XRD. This agrees with the analysis of the chemical composition of the CNC, where silicon dioxide (SiO_2) was found to naturally occur as quartz and its melting point being 1713°C. Thus the calcination temperature of the sample studied did not undergo any change.

Figure 8 shows the image obtained by SEM of a part of the calcined sample. Point 20 indicates a grain of Albite, one of the crystalline phases that was not partially destroyed during the calcination process.

In the microprobe analysis, the typical elements of the albite formula are detected (Phillips and Griffen, 1981), forming aluminum and sodium silicates, in this case of partial substitutions of sodium by calcium. In the calcined sample, according to the criteria of Armbruster et al. (1990), the albite is a facilitator of the fusion of clays, with which it has formed a ceramic material that serves as glue to join the rest of the highly refractory phases that have been detected.

In Figure 8, point 21 shows a quartz grain, which was previously mentioned and at the point marked with the number 23, a hornblende grain, one of the phases that was also detected in the calcined clay.

XRD

Another of the phases detected by XRD was Muscovite, which in Figure 8 appears marked by point 23 and in Figure 9, it reproduces with a greater increase. In the microprobe analysis that is attached, the presence of the elements present in the Muscovite formula can be identified. As described, in the topochemical reactions that occurred during the calcination process, the albite partially served as

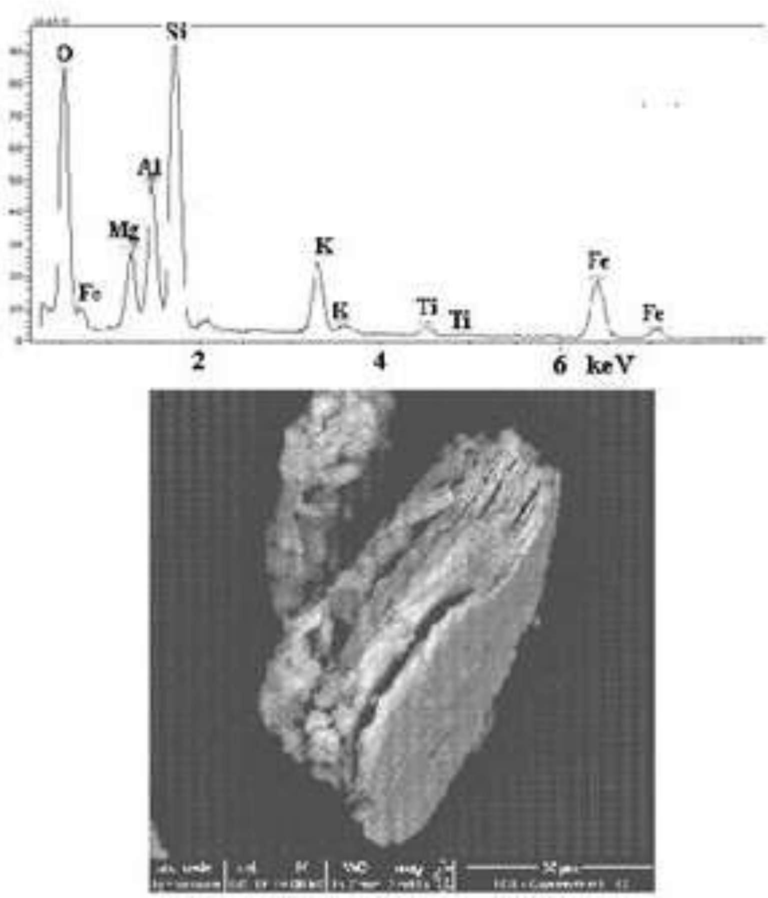

Figure 9: Muscovite phase in CCNC by SEM.

a flux and accelerated the fusion of the clay, whose products formed the glue that holds together the mentioned phases. Higher melting than the calcination temperature retained their crystalline structure. Most of the phases present in the products of the calcination of the clay studied correspond to ceramic materials of high hardness (Brindley and Brown, 1980), which have suitable properties to be used as reinforcements of metal matrix composite materials such as aluminum matrix.

Conclusions

The basic conclusions are summarized as follows:

1. The SCBA, collected directly from the boiler and crushed, has a fine granulometry with grain diameter between 0.7 and 130 μm and average diameter (D50) of 34.97 μm. It is basically formed by silica, in concentrations of approximately 80% . The Cristobalite and the tridymite are the main crystalline phases present in this ash. The phasic characterization of SCBA by XRD also shows the presence of potassium and magnesium silicates.
2. The CNC from the Miller deposit in Villa Clara, is a kaolinite, in which montmorillonite and illite are also found. Meanwhile, using techniques of XRD, SEM and microprobe in the CCNC during 4h at a temperature of 1000°C, the quartz, magnesium-hornblende, diopside, albite and muscovite phases could be characterized.
3. Both the SCBA collected directly from the boiler and the CCNC, being constituted by phases of the ceramic type, constitute excellent candidates to be used as reinforcement materials for metal matrix compounds, in particular aluminum matrix.2.

REFERENCES

Alaneme KK, Adewuyi EO (2013). Mechanical Behaviour of AL-MG-SI Matrix Composites Reinforced with Alumina and Bamboo Leaf ash. Metall. Mater. Eng. 19(3): 177-187.

Anas M, Khan MZ (2015). Comparison of hardness and strength of fly ash and bagasse ash Al-MMCs. IJSART, 1(7): 88-93.

Armbruster T, Burgi HB, Kunz M, Gnos E, Bronnimann S, Lienert C (1990). Variation of displacement parameters in structure refinements of low albite. Am. Mineral. 75: 135-140.

Asavavisithchai S, Tantisiriphaiboon R (2009). On the Production of Aluminium Foams Stabilised Using Particles of Rice Husk Ash. Chiang Mai J. Sci. 36(3): 302-311.

Brindley GM, Brown G (1980). Cristal structures of clay minerals and their X-ray identifications - Mineralogical Society. London, 495 pp.

Fatile OB, Akinruli JI, Amori AA (2014). Microstructure and mechanical behaviour of stir-cast Al-Mg-Sl alloy matrix hybrid composite reinforced with corn cob ash and silicon carbide. Int. J. Eng. Technol. Innov. 4(4): 251-259.

Itskos G, Moutsatsou A, Rohatgi PK, Koukouzas N, Vasilatos C, Katsika E (2011). Compaction of High-Ca Fly Ash-Al and Al-Alloy-Composites: Evaluation of their Microstructure and Tribological Performance. Coal Combust. Gasification Prod: 3: 75-82, (2011).

Jyothi PN, Bharath Kumar BS (2015). Comparison of Mechanical Properties of Al-5%Si Alloy Reinforced with Cow dung ash and Rice husk ash Int. J. Latest Res. Eng. Technol. (IJLRET) 1(4): 55-58.

Kamat SV, Hirth JP, Mehrabian R (1989). Mechanical properties of particulate-reinforced aluminum-matrix composites. Acta Metall. 37(9): 2395-2402.

Lancaster LM, Lung H, Sujan D (2013). "Utilization of Agro-Industrial Waste in Metal Matrix Composites: Towards Sustainability". Int. J. Environ. Chem. Ecol. Geol. Geophys. Eng. 7(1): 35-43.

Lloyd DJ(1994). Particle reinforced aluminium and magnesium matrix composites. Int. Mat. Rev. 39(1).

Phillips WR, Griffen DT (1981). OpticalMineralogy. W.H. Freeman & Co.

Saravanan SD, Senthilkumar M (2014). Mechanical Behavior of Aluminum ($AlSi_{10}Mg$)-RHA Composite. Int. J. Eng. Technol. 5(6): 4834- 4840.

Subrahmanyam APSVR, Narsaraju G, Rao BS (2015). Effect of Rice Husk ash and Fly ash Reinforcements on Microstructure and Mechanical properties of Aluminium alloy ($AlSi_{10}Mg$) Matrix Composites. Int. J. Adv. Sci. Technol. 76: 1-8.

Surappa MK (2003). Aluminium matrix composites: Challenges and opportunities. Sadhana, 28(1-2): 319-334.

Villar-Cociña E, Frías M, Hernández-Ruiz J, Savastano H Jr. (2013). Pozzolanic behavior of a bagasse ash coming from the boiler of a Cuban sugar factory. Adv. Cement Res. 25(3).

Wade A, Mattox RB (1976). Elementos de cristalografía y mineralogía, Ed. Omega, Traducción de la 2ª edición. Barcelona.

Włodarczyk-Fligier A, Dobrzański LA, Kremzer M, Adamiak M (2008). Manufacturing of aluminium matrix composite materials reinforced by Al_2O_3 particles. J. Achiev. Mater. Manuf. Eng. 27(1): 99-102.

Zuhailawati H, Samayamutthirian P, MohdHaizu CH (2007). Fabrication of Low Cost Aluminium Matrix Composite Reinforced with Silica Sand. J. Phys. Sci. 18(1): 47-55.

Cite this article as:

Pino-Rivero L, Hernández-Ruiz JE, Villar-Cociña E, Alujas Díaz A (2018). "Characterization of industrial pollutant waste materials and clays for possible use as reinforcement in aluminum matrix composite". Acad. J. Environ. Sci. 6(8): 185-193.

Submit your manuscript at
http://www.academiapublishing.org/journals/ajes